

Chemical genetic analysis of the budding-yeast p21-activated kinase Cla4p

Eric L. Weiss*, Anthony C. Bishop†, Kevan M. Shokat‡ and David G. Drubin*§

*Department of Molecular and Cell Biology, University of California, Berkeley, California 94720-3202, USA

†Department of Chemistry, Princeton University, Princeton, New Jersey 08544, USA

‡Department of Cellular and Molecular Pharmacology, University of California, San Francisco, California 94143, USA

§e-mail: drubin@uclink4.berkeley.edu

The p21-activated kinases (PAKs) are effectors for the Rho-family GTPase Cdc42p. Here we define the *in vivo* function of the kinase activity of the budding yeast PAK Cla4p, using *cla4* alleles that are specifically inhibited by a cell-permeable compound that does not inhibit the wild-type kinase. *CLA4* kinase inhibition in cells lacking the partially redundant PAK Ste20p causes reversible *SWE1*-dependent cell-cycle arrest and gives rise to narrow, highly elongated buds in which both actin and septin are tightly polarized to bud tips. Inhibition of Cla4p does not prevent polarization of F-actin, and cytokinesis is blocked only in cells that have not formed a bud before inhibitor treatment; cell polarization and bud emergence are not affected by Cla4p inhibition. Although localization of septin to bud necks is restored in *swe1Δ* cells, cytokinesis remains defective. Inhibition of Cla4p activity in *swe1Δ* cells causes a delay of bud emergence after cell polarization, indicating that this checkpoint may mediate an adaptive response that is capable of promoting budding when Cla4p function is reduced. Our data indicate that *CLA4* PAK activity is required at an early stage of budding, after actin polarization and coincident with formation of the septin ring, for early bud morphogenesis and assembly of a cytokinesis site.

Rho-family GTPases control cell morphology and participate in signal-transduction cascades in a wide range of eukaryotes¹. Some rho-family GTPases bind to and activate members of the broadly distributed family of PAKs; these enzymes have been implicated in actin organization and polarity development in several cell types². In *Saccharomyces cerevisiae*, the Rho-family GTPase Cdc42p is required for cell polarization in the G1 phase^{3,4}. Polarization of the actin cytoskeleton in G1 presages the emergence of a daughter bud. Construction of the cytokinesis site at the narrow bud neck between mother and daughter cells begins concurrently with budding, with the deposition of a filament system composed of evolutionarily conserved proteins known as septins. Although the localization of septins to the neck of the emerging bud is clearly an important part of morphogenesis of the cytokinesis site^{5,6}, the functional relationship between their spatial organization and the mechanics of cytokinesis has not been established. In fact, cytokinesis occurs in cells in which the septin-filament structure is considerably disrupted^{7,8}.

Ste20p and Cla4p are PAKs that redundantly carry out undefined functions that are essential for viability. They bind to and are activated by Cdc42p, and are thus attractive candidates for effectors of Cdc42p in cytoskeleton organization^{9–12}. Skm1p, a protein that is similar to Cla4p, is apparently not capable of carrying out these functions¹³. Previous results indicate that Ste20p and Cla4p may have diverse functions in organization of the actin cytoskeleton. Permeabilized *cdc42-1* cells nucleate the assembly of F-actin poorly *in vitro*; *ste20Δ* and *cla4Δ* cells are similarly impaired in this activity, a striking result given that the latter strains do not exhibit pronounced defects in actin polarization. Addition of Ste20p restores this *in vitro* nucleation¹⁴. A temperature-sensitive *cla4-75* allele exhibits defects in bud and bud-neck morphology, but not in G1 actin polarization¹⁰. Attachment of a 'ts degron' domain, which causes proteins to be degraded at 37 °C, to the *cla4-75* protein, has been reported to conditionally block actin polarization throughout the cell cycle¹⁵. However, the biochemical defects that give rise to these phenotypes are obscure. Furthermore, the phenotypes of any

conditional allele must be judged against the physiological effects of the restrictive conditions. In wild-type yeast cells, heat shock causes rapid, *RHO1*-mediated depolarization of the actin cytoskeleton, presumably in response to cell-wall stress; repolarization is partially dependent on the activity of protein kinase C¹⁶. Budding yeast probably possess adaptive mechanisms that ensure functional actin organization under varying conditions — the Cdc42p-binding proteins encoded by *GIC1* and *GIC2*, for example, are only essential for actin polarization at 37 °C, whereas the proteins encoded by *MSB3* and *MSB4* are important at lower temperatures^{17–19}. The phenotypes of temperature-conditional alleles could therefore indicate either a general function of the affected gene product in cytoskeleton organization, or a more specialized role in adaptation to a subset of conditions experienced by free-living microbes.

Results

Construction of analogue-sensitive *cla4* alleles. To rapidly and isothermally inhibit the kinase activity of Cla4p, we constructed three analogue-sensitive (*as*) *cla4* alleles that confer differing degrees of sensitivity to the PP1 (4-amino-1-tert-butyl-3-(p-methylphenyl)pyrazolo[3,4-d]pyrimidine) derivative 1NM-PP1 (4-amino-1-tert-butyl-3-(1-naphthylmethyl)pyrazolo[3,4-d]pyrimidine; ref. 20). The substitutions we introduced to create the *cla4-as1* and *cla4-as2* alleles (Fig. 1a) are homologous to substitutions in the *src*-encoded protein kinase that confer highly specific sensitivity to PP1 derivatives^{20–22}. We constructed the *cla4-as3* allele (Fig. 1a) in the hope of increasing the sensitivity of the *cla4-as2* allele to inhibition by PP1 derivatives. Our rationale for constructing this allele was based on the crystal structures of the *src*- and *hck*-encoded protein kinases complexed with PP1, which indicate that amino acids immediately amino-terminal to the conserved DFG motif in kinase subdomain 7 may participate in binding to PP1 and its derivatives²³. Although this side chain is relatively small in many kinases, several other protein kinases have larger amino acids at this

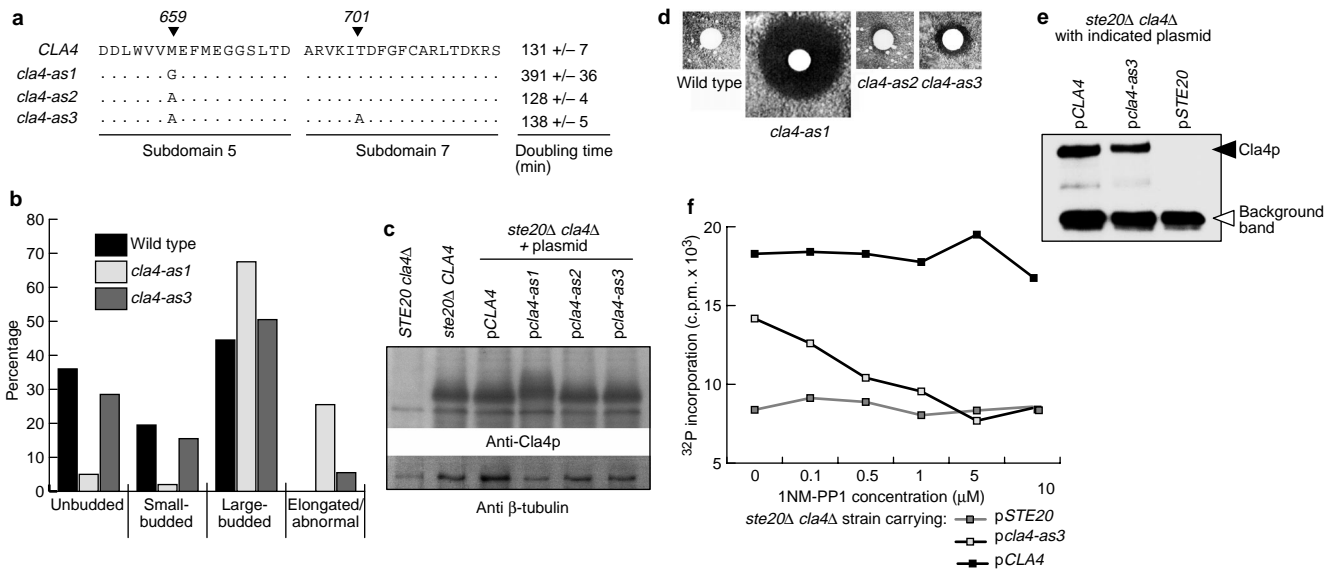


Figure 1 *cla4* alleles that confer sensitivity to 1NM-PP1. **a**, Mutant *cla4* alleles that confer sensitivity to 1NM-PP1. Amino-acid numbers are shown above the sequences. The doubling time of a $\Delta ste20 \Delta cla4$ strain carrying the corresponding allele on a plasmid in YPD medium at 25 °C is shown adjacent to the allele sequence. **b**, Distribution of different budding morphologies in *ste20Δ cla4Δ* strains carrying pCLA4 (wild type, black bars), pcla4-as1 (*cla4 as1*, open bars), or pcla4-as3 (*cla4-as3*, filled bars) grown at 25 °C. **c**, Expression of Cla4p in a *cla4Δ* strain (DDY2050), a *ste20Δ* strain (DDY2051) and *ste20 Δ, cla4 Δ* strains carrying CLA4 alleles on a low-copy centromeric plasmid (DDY2053–2056). Upper panel,

immunoblot against Cla4p; lower panel, corresponding anti-β-tubulin immunoblot. **d**, Filter discs spotted with 12 μl of 750 μM 1NM-PP1 placed onto uniform lawns of wild-type (DDY2053), *cla4-as1* (DDY2054), *cla4-as2* (DDY2055) and *cla4-as3* (DDY2056) cells. **e**, Immunoblot against Cla4p immunoprecipitated from wild-type (DDY2053), *cla4-as3* (DDY2056) and *STE20* (DDY2052) strains. Filled arrow denotes Cla4p, open arrow denotes background band of relative molecular mass ~58,000, which is distinct from the immunoglobulin signal. **f**, Phosphorylation of myelin basic protein by Cla4p immune complexes in the presence of increasing concentrations of 1NM-PP1. IP, immunoprecipitation.

position — Cla4p has threonine. We surmised that introducing a smaller amino acid at this position might enhance binding of PP1 derivatives.

***cla4-as* alleles confer sensitivity to 1NM-PP1.** Plasmid-borne copies of *cla4-as* alleles complemented a *ste20Δ cla4Δ* double-mutant strain to varying degrees (strains DDY2054–2056). The doubling rate of *ste20Δ cla4Δ* cells expressing *cla4-as1* was much lower than normal (Fig. 1a), and the majority of these cells possessed abnormally large buds or exhibited aberrant morphology (Fig. 1b). In contrast, the *cla4-as2* and *cla4-as3* alleles allowed growth at rates that were similar to that of wild-type *CLA4* (Fig. 1a). There was, however, a slight bias towards large-budded cells and a small fraction of cells with abnormal morphology in *ste20Δ cla4Δ* strains carrying *cla4-as2* or *cla4-as3* alleles (Fig. 1b). Levels of Cla4p in strains carrying *CLA4* and *cla4-as* alleles on centromeric plasmids were similar to those in a strain carrying the endogenous *CLA4* allele (Fig. 1c), indicating that the plasmid-borne mutant alleles were not overexpressed. The electrophoretic mobility of the *cla4-as1* protein on an SDS–polyacrylamide gel (Fig. 1c, lane 4) seemed to be retarded relative to those of the other variants (Fig. 1c.).

Whereas growth of *ste20Δ cla4Δ* cells carrying plasmid-borne *CLA4* was not inhibited by 1NM-PP1 on solid medium, we found that *cla4-as* alleles imparted sensitivity to 1NM-PP1 — *cla4-as1* conferred the greatest sensitivity, *cla4-as3* conferred intermediate sensitivity and *cla4-as2* conferred only slight sensitivity (Fig. 1d). As *cla4-as3* complemented *ste20Δ cla4Δ* adequately and conferred sensitivity to 1NM-PP1, we used this allele for further analysis. For brevity, we hereafter refer to *ste20Δ cla4Δ, pcla4-as3* (strain DDY2056) as '*cla4-as3*' and *ste20Δ cla4Δ, pCLA4* (strain DDY2053) as the wild type (Table 1). Strains of similar genotype carrying chromosomally integrated copies of *cla4-as* alleles were essentially phenotypically identical to the strains carrying the alleles on a centromeric plasmid, both in doubling time and in sensitivity to

1NM-PP1 (data not shown). We found that deletion of *SKM1* did not affect the phenotypes of *cla4-as3* strains (data not shown).

To assess the effect of 1NM-PP1 on the *in vitro* kinase activity of Cla4p, we carried out protein-kinase assays with Cla4p immunoprecipitated from wild-type and *cla4-as3* strains, using myelin basic protein as a substrate²⁴. For negative control precipitations, we used a related strain in which *CLA4* is not expressed (*ste20Δ cla4Δ, pSTE20*; strain DDY2052). We were able to immunoprecipitate similar amounts of Cla4p from extracts of wild-type and *cla4-as3* cells (Fig. 1e). The *in vitro* protein-kinase activity of immunoprecipitated wild-type protein was lower than that of immunoprecipitated *cla4-as3* protein, although significantly higher than control kinase-activity levels. Addition of 1NM-PP1 to *in vitro* assays resulted in inhibition of kinase activity associated with *cla4-as3* immunoprecipitates, but had little effect on kinase activity of immunoprecipitates from both negative control and wild-type strains (Fig. 1f). Inhibition of the kinase activity of *cla4-as3* was dependent on the concentration of 1NM-PP1 added; the IC₅₀ value was ~240 nM. These assays indicate that 1NM-PP1 is capable of inhibiting the enzymatic activity of the *cla4-as3*-encoded protein at concentrations that do not detectably inhibit wild-type Cla4p.

Phenotypic effect of Cla4p inhibition. Addition of 1NM-PP1 to *cla4-as3* cultures caused a profound, dose-dependent effect on cell morphology. As the concentration of 1NM-PP1 increased, we found that an increasing fraction of cells had narrow, highly elongated buds (Fig. 2a, b; maximal at ≥25 μM 1NM-PP1). F-actin was concentrated at the tips of these elongating buds (Fig. 2b), which became longer over time without a corresponding increase in the size of the mother cell (data not shown). The nuclei of these cells were undivided, located close to the bud neck (Fig. 2b), and uniformly contained short bipolar mitotic spindles (data not shown). Levels of Cla4p were not affected by addition of 1NM-PP1 to *cla4-as3* cells; however, a fraction of the protein exhibited retarded electrophoretic mobility

Table 1 Yeast strains

Strain name	Genotype
DDY759*	<i>MATa, ura3-1/ura3-1, trp1-1/trp1-1, ade2-1/ade2-1, leu2-3,112/leu2-3,112, his3/his3</i> (W303 background strain)
DDY2050	<i>MATa, cla4Δ::LEU2, ura3-1, trp1-1, ade2-1, leu2-3,112, his3</i>
DDY2051	<i>MATa, ste20Δ::KanMX, ura3-1, trp1-1, ade2-1, leu2-3,112, his3</i>
DDY2052	<i>MATa, ste20Δ::KanMX, cla4Δ::LEU2, ura3-1, trp1-1, ade2-1, leu2-3,112, his3, pRS316-STE20</i>
DDY2053	<i>MATa, ste20Δ::KanMX, cla4Δ::LEU2, ura3-1, trp1-1, ade2-1, leu2-3,112, his3, pYEpLac24-CLA4</i>
DDY2054	<i>MATa, ste20Δ::KanMX, cla4Δ::LEU2, ura3-1, trp1-1, ade2-1, leu2-3,112, his3, pYEpLac24-cla4-as1</i>
DDY2055	<i>MATa, ste20Δ::KanMX, cla4Δ::LEU2, ura3-1, trp1-1, ade2-1, leu2-3,112, his3, pYEpLac24-cla4-as2</i>
DDY2056	<i>MATa, ste20Δ::KanMX, cla4Δ::LEU2, ura3-1, trp1-1, ade2-1, leu2-3,112, his3, pYEpLac24-cla4-as3</i>
DDY2057	<i>MATa, ste20Δ::KanMX, cla4Δ::LEU2, swe1Δ::hisGXM3, ura3-1, trp1-1, ade2-1, leu2-3,112, his3, pYEpLac24-cla4-as3</i>
DDY2058	<i>MATa, ste20Δ::KanMX, cla4Δ::LEU2, URA3::GFP-CDC3, trp1-1, ade2-1, leu2-3,112, his3, pYEpLac24-CLA4</i>
DDY2059	<i>MATa, ste20Δ::KanMX, cla4Δ::LEU2, URA3::GFP-CDC3, trp1-1, ade2-1, leu2-3,112, his3, pYEpLac24-cla4-as3</i>
DDY2060	<i>MATa, ste20Δ::KanMX, cla4Δ::LEU2, URA3::cla4-75-ts degron, trp1-1, ade2-1, leu2-3,112, his3</i>
DDY2061	<i>MATa, ste20Δ::KanMX, cla4Δ::LEU2, URA3::cla4-75-ts degron, trp1-1, ade2-1, leu2-3,112, his3, pYEpLac24-CLA4</i>
DDY2062	<i>MATa, ste20Δ::KanMX, cla4Δ::LEU2, URA3::cla4-75-ts degron, trp1-1, ade2-1, leu2-3,112, his3, pYEpLac24-cla4^{D693A}</i>
KBY212**	<i>MATα, ste20Δ::ΔDE2, cla4Δ::LEU2, URA3::cla4-75-ts degron, trp1-1, ade2-1, leu2-3,112</i>
DDY2063	<i>MATα, ste20Δ::ΔDE2, cla4Δ::LEU2, URA3::cla4-75-ts degron, trp1-1, ade2-1, leu2-3,112, pYEpLac24-CLA4</i>
DDY2064	<i>MATα, ste20Δ::ΔDE2, cla4Δ::LEU2, URA3::cla4-75-ts degron, trp1-1, ade2-1, leu2-3,112, pYEpLac24-cla4^{D693A}</i>

*Provided by A. Sachs; **provided by K. Blumer. All other strains were generated for this study.

with increasing duration of exposure to inhibitor (Fig. 2c). Although it is not known whether this shift represents the same modifications, Cla4p has been found to be phosphorylated in M phase and in response to expression of hyperactivated Cdc42p²⁴. As we observed neither altered electrophoretic mobility of Cla4p nor increased frequency of aberrant cell morphologies in 1NM-PP1-treated wild-type cells, we conclude that these effects are the result of *in vivo* inhibition of *cla4-as3* kinase activity. To examine the effects of *CLA4* kinase inhibition at increased temperatures, we compared the phenotypes of *cla4-as3* cells treated with 1NM-PP1 at 25 °C and 37 °C. Whereas the majority of *cla4-as3* cells treated with 1NM-PP1 at 25 °C had highly polarized, elongated buds (Fig. 2b), the same treatment at 37 °C yielded cells with large, round buds and depolarized actin (Fig. 2d; 76.5%, *n* = 200). At both temperatures, budded cells each contained a single nucleus, which is consistent with cell-cycle arrest. The marked difference in bud morphology at 37 °C indicates either that Cla4p kinase activity may be required for persistent polarization of F-actin at increased temperatures, or that this type of cell polarization may be inherently temperature-sensitive. However, these experiments do not address the possibility that the pharmacology of *cla4-as3* inhibition is different at increased temperatures.

Inhibition of the kinase activity of Cla4p affects organization of septins within budded cells. We examined the localization of a variant of Cdc3p that is fused to green fluorescent protein (GFP) at its carboxy terminus (strains DDY2058 and 2059), and localized the septin Cdc11p using a polyclonal anti-Cdc11p antibody. Within 1 h of addition of 1NM-PP1 to *cla4-as3* cells, we found that the septins Cdc3p and Cdc11p were distributed throughout the buds of small-budded cells — in wild-type cells of similar morphology, these proteins most frequently localized to a band at the bud neck (Fig. 2e). As the buds of 1NM-PP1-treated *cla4-as3* cells elongated, Cdc3p and Cdc11p remained localized as a cortical cap at the tips of elongating buds. Some septin was present at the mother–daughter bud neck in most cells (77.5%, *n* = 200 budded cells). Of cells in which septin was present at the bud neck, 26% had a bright, narrow band similar to those in wild-type cells, 53% had continuous bands around an unusually wide bud neck, and 21% had partial

rings and wide bud necks. A fraction of cells also exhibited spots of septin localization along highly elongated buds; we did not observe complete rings at these sites in any cells. These results indicate that hyperpolarized bud growth induced by loss of Cla4p kinase activity is accompanied by marked redistribution of septins from their normal location to sites of polarized growth, although the causal relationship is not clear.

Cla4p inhibition does not affect cytokinesis if buds have emerged, and does not block bud emergence. Cla4p has been reported to function in bud emergence and cytokinesis. To define more precisely the stage of cell division at which Cla4p kinase activity is required, we examined the effects of 1NM-PP1 treatment on cells at various stages of the cell cycle. To examine the effect of Cla4p inhibition on cells that had budded before exposure to 1NM-PP1, we synchronized cultures with hydroxyurea, which causes cells to remain in S phase with large, round buds, and released cells from this arrest into media in the presence or absence of the inhibitor. The percentage of cells with large, round buds fell at similar times after release in all cultures, indicating that the execution of cytokinesis was unaffected by 1NM-PP1 treatment (Fig. 3a). Wild-type and untreated *cla4-as3* cells subsequently formed normal round buds, whereas the buds of 1NM-PP1-treated *cla4-as3* cells were uniformly elongated (data not shown). These results indicate that the kinase activity of Cla4p may not be required for cytokinesis once the bud neck has been properly formed.

To assess the function of Cla4p kinase activity in bud emergence, we examined the budding of single cells and synchronized cultures. To examine the behaviour of single cells, we used a micromanipulator to group individual wild-type and *cla4-as3* cells on plates containing 30 μM 1NM-PP1 according to initial morphology. All *cla4-as3* cells that initially possessed small buds grew daughter buds with normal morphology (100/100); after division, the resulting cells then grew elongated buds (189/200). In contrast, the majority (88/100) of initially unbudded *cla4-as3* cells formed single, elongated buds. The remainder (12/100) budded normally and divided; all daughters of these cells subsequently formed elongated buds. Wild-type cells budded normally in the presence of the inhibitor. These results indicate that the kinase activity of Cla4p may be required for

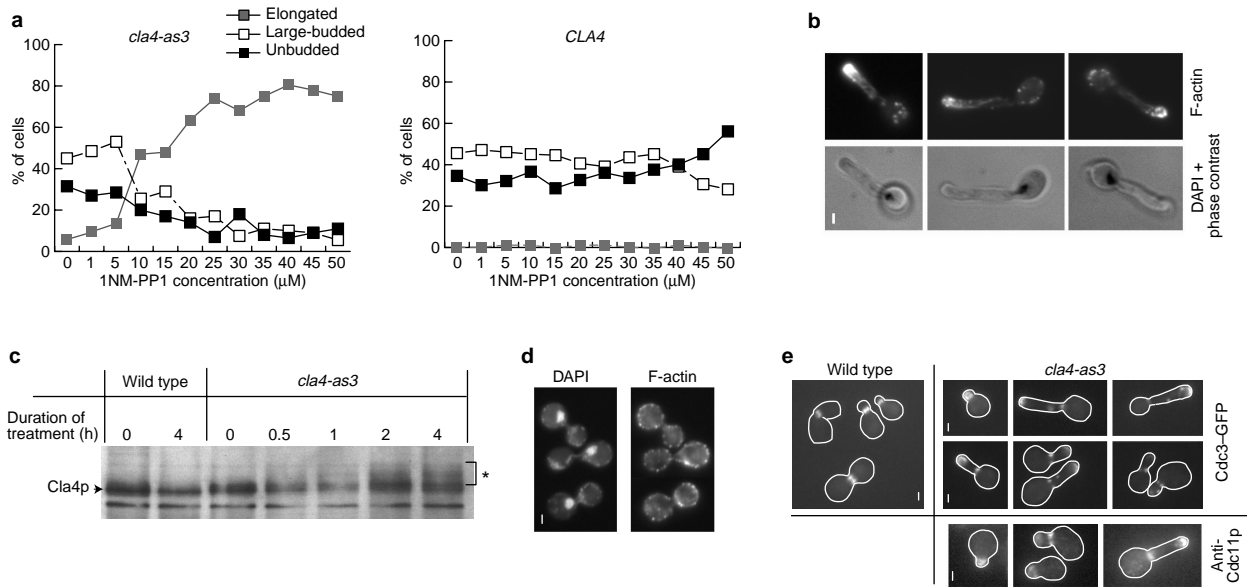


Figure 2 Phenotypes associated with inhibition of Cla4p. **a**, Dose-response pharmacology of 1NM-PP1 treatment. Left panel, distribution of different budding morphologies in *cla4-as3* (DDY2056) cells treated with increasing concentrations of 1NM-PP1 for 4 h; right panel, distribution of different budding morphologies in similarly treated wild-type (DDY2052) cells. Grey boxes represent cells with narrow elongated buds; black boxes represent unbudded cells; open boxes represent large-budded cells. Small-budded cells are excluded for clarity. **b**, Morphology of 1NM-PP1-treated *cla4-as3* cells. Upper panels, F-actin (stained with rhodamine-phalloidin); lower panels, corresponding superimposed staining of DNA (DAPI) and

phase-contrast images. Scale bar represents 1 μm. **c**, Modification of *cla4-as3*-encoded protein upon treatment with 1NM-PP1. **d**, Morphology of *cla4-as3* cells treated with 1NM-PP1 at 37 °C. Left panel, staining of DNA (DAPI); right panel, corresponding F-actin staining (rhodamine-phalloidin). Scale bar represents 1 μm. **e**, Septin organization in response to inhibition of Cla4p. Upper panels, GFP fluorescence of 1NM-PP1-treated wild-type and *cla4-as3* cells carrying an integrated *CDC3* gene C-terminally fused to the coding sequence for GFP. Lower panels, anti-Cdc11p immunofluorescence of 1NM-PP1-treated *cla4-as3* cells. Scale bar represents 1 μm.

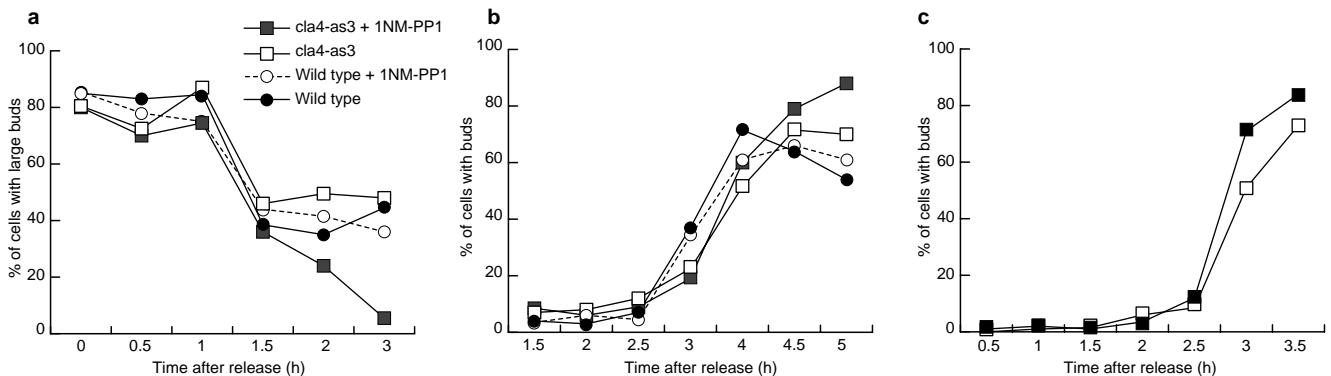


Figure 3 Effect of Cla4p inhibition on cytokinesis and bud emergence. Dark grey boxes and lines represent 1NM-PP1-treated *cla4-as3* cultures; light grey boxes and lines represent untreated *cla4-as3* cultures; open circles and dashed lines represent 1NM-PP1-treated wild-type cells; filled black circles and solid lines represent untreated wild-type cells. **a**, Percentage of cells with large buds in cultures released

from hydroxyurea (stationary-phase) arrest. Elongated buds were not scored as large buds. **b**, Percentage of cells with buds of any morphology in cultures after release from stationary-phase arrest. **c**, Percentage of cells with buds of any morphology; cells were synchronized by centrifugal elutriation.

bud morphogenesis only before buds have emerged. We also synchronized *cla4-as3* cells by enrichment of unbudded cells from stationary-phase cultures²⁵ and by centrifugal elutriation²⁶, releasing in the presence or absence of 1NM-PP1. Perhaps surprisingly, treatment of *cla4-as3* cells with 1NM-PP1 did not significantly delay bud emergence in the G1 phase at 25 °C (Fig. 3b, c). The buds of synchronized, 1NM-PP1-treated *cla4-as3* cells were uniformly elongated (data not shown). These results place the execution point for

Cla4p inhibition at or before an early stage of bud emergence.

These results indicate that the kinase activity of Cla4p may not be required for polarization of the actin cytoskeleton, and stand in contrast to some phenotypes associated with depletion of Cla4p at increased temperatures¹⁵. One possible explanation for this difference is that the protein has functions that are independent of its kinase activity. We tested this possibility by expressing wild-type and kinase-inactive forms of Cla4p in both the *cla4-75-ts* degenon

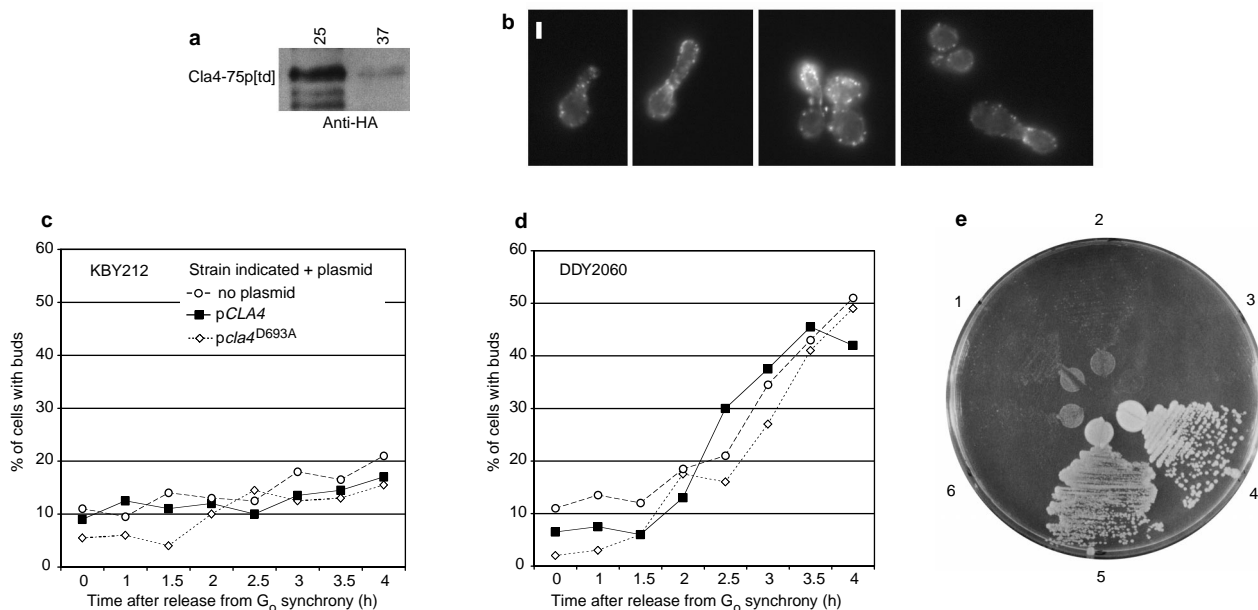


Figure 4 Phenotypic variation among *cla4-75* ts degron strains. a. Immunoblot against the haemagglutinin (HA) epitope, showing levels of degron-tagged Cla4p in an independently constructed *cla4-75* ts degron strain, upon shift to 37 °C after induction of the degron-tagged protein at 25 °C with Cu²⁺ as described¹⁵. **b.** Budding phenotype of the *cla4-75* ts degron strain 6 h after release from stationary-phase arrest at 37 °C. Scale bar represents 2 μm. **c, d.** Kinetics of bud emergence in the *cla4-75* ts degron strains KBY212 (**c**, ref. 15), DDY2063 (**d**), and isolates of these strains carrying either *CLA4* or *cla4*^{D693A} on a centromeric

plasmid. Circles with dashed lines represent strains carrying no plasmid; squares with solid lines represent strains carrying pCLA4 (a centromeric plasmid bearing the wild-type *CLA4* gene); diamonds with dashed lines represent strains carrying p*cla4*^{D693A} (a centromeric plasmid bearing the *cla4*^{D693A} allele). **e.** Plate showing complementation of different *cla4-75* ts degron strains by wild-type *CLA4* at 37 °C. Sector 1, KBY212 carrying no plasmid; sector 2, KBY212 carrying pCLA4; sector 3, KBY212 carrying p*cla4*^{D693A}; sector 4, DDY2053 (pCLA4, no degron construct); sector 5, DDY2063 carrying pCLA4; sector 6, DDY2053 carrying no plasmid.

strain (KBY212; ref. 15) and in a *cla4-75*-ts degron strain we constructed (DDY2060) using the same approach^{15,27}. At 37 °C, the degron-tagged protein was degraded in strain DDY2060, as reported for KBY212 (Fig. 4a). However, the strain DDY2060 exhibited an abnormal budding morphology at restrictive temperature (Fig. 4b), and did not suffer an absolute block of bud emergence as reported for KBY212 when released from stationary-phase block (Fig. 4c, d). We found that KBY212 was very poorly complemented by a centromeric plasmid carrying the wild-type *CLA4* allele (Fig. 4c, e, sector 2). In contrast, DDY2060 was effectively complemented by this construct (Fig. 4c, e, sector 4). The catalytically inactive *cla4*^{D693A} mutant²⁴ did not complement either KBY212 or DDY2060 (Fig. 4c–e, data not shown). The presence of this allele seemed to reduce further the growth of both strains at 37 °C, but did not significantly affect the kinetics of budding in either strain (Fig. 4b, c, sector 3 and data not shown), and did not significantly change the budding morphology of DDY2060 (data not shown). Hence, we were unable to use these strains to assess the possibility that the *CLA4*-encoded protein has functions that are independent of its kinase activity in actin organization. It is possible that the *cla4-75*-ts degron protein exerts a dominant effect in the KBY212 genetic background that is absent in the DDY2060 background. Alternatively, the KBY212 strain may contain a second mutation that impairs its growth at increased temperatures.

Elimination of the *SWE1*-dependent checkpoint alters the Cla4p-inhibition phenotype. The protein encoded by *SWE1* has been proposed to control a ‘morphogenesis checkpoint’ that induces arrest of the cell cycle in response to disruption of septin-filament structure, cell polarity, or F-actin organization^{28,29}. Deletion of *SWE1* in *cla4-as3* cells (strain DDY2057) markedly altered the phenotype

caused by addition of 1NM-PP1. Upon addition of inhibitor, a large fraction of *cla4-as3 swe1Δ* cells became multinucleated and developed several buds (Fig. 5a); these buds were not elongated, and septins were generally localized to bud necks (Fig. 5b). This strain also had a significant fraction of morphologically abnormal cells in the absence of inhibitor (Fig. 5a). To eliminate the complication introduced by these cells of variable abnormal morphology, we obtained an almost uniformly unbudded population of *cla4-as3 swe1Δ* cells by centrifugal elutriation and added various concentrations of 1NM-PP1 to them. Untreated *cla4-as3 swe1Δ* cells began to bud ~2.5 h after release from this synchrony at 25 °C (Fig. 5c). Actin was polarized appropriately in these cells upon budding, and septins were localized to the bud necks of most cells (Fig. 5e, f). Septin organization was occasionally abnormal in untreated *cla4-as3 swe1Δ* cells (Fig. 5f). However, there was not a marked increase in the incidence of multibudded and multinucleated cells (Fig. 5d), indicating that there was not widespread mis-segregation of nuclei or failure of cytokinesis in untreated cells.

Addition of 1NM-PP1 to elutriated *cla4-as3 swe1Δ* cells resulted in a concentration-dependent delay in bud emergence. At 5 μM 1NM-PP1, bud emergence was only slightly retarded, whereas concentrations above 25 μM caused a more pronounced delay (Fig. 5c). To determine whether this delay was due to failure of cell polarization, we analyzed the distribution of F-actin and the septin Cdc11p in *cla4-as3 swe1Δ* cells treated with 25 μM and 50 μM 1NM-PP1. Asymmetric distribution of both actin and the septins was evident in these cells at similar times; the foci of actin and septin were coincident (Fig. 5e). F-actin, though clearly polarized in 1NM-PP1-treated cells, was frequently not as closely constricted to the presumptive bud site as in untreated cells (Fig. 5e, asterisk). There was

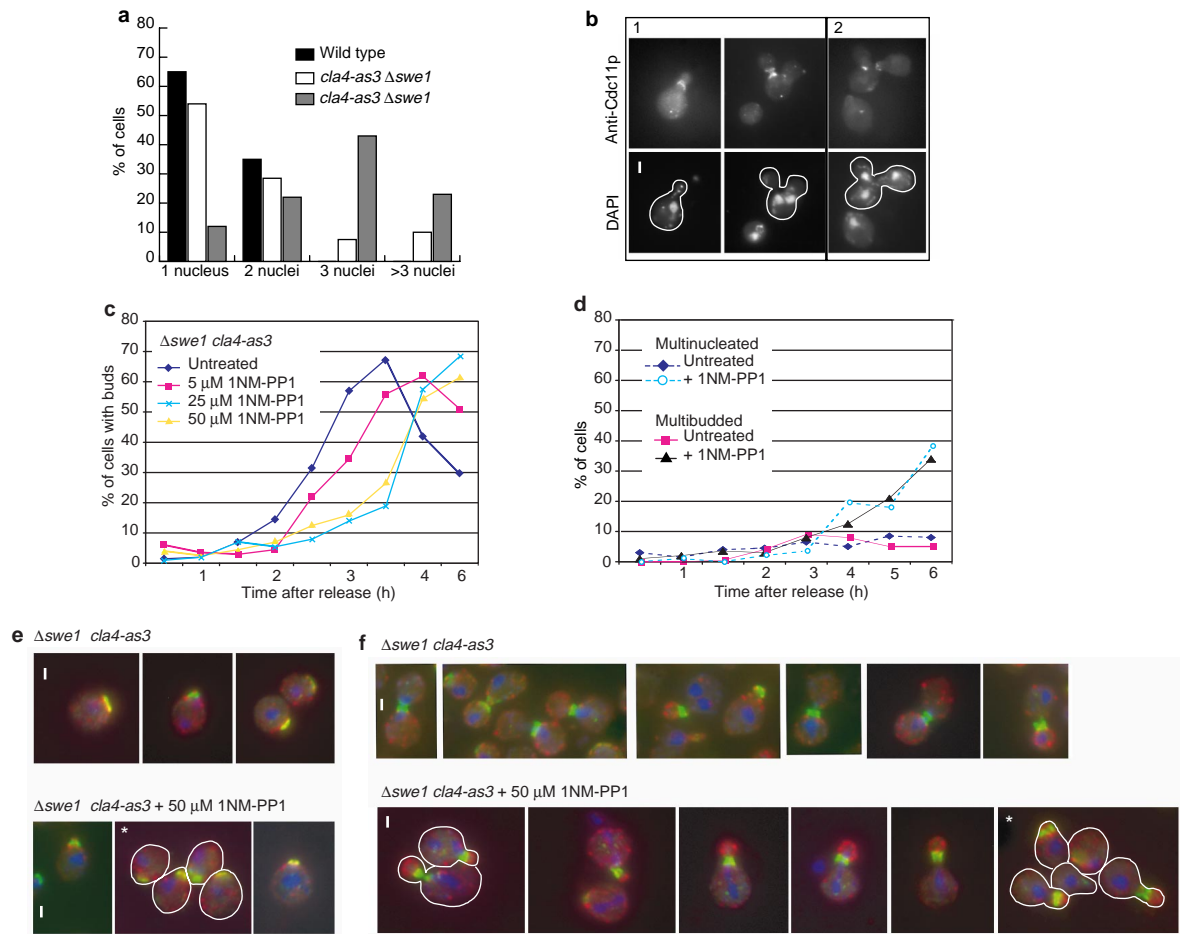


Figure 5 Phenotype of 1NM-PP1-treated *cla4-as3 swe1Δ* cells. **a**, Graph showing the number of nuclei in untreated and inhibitor treated *cla4-as3 swe1Δ* cells (strain DDY2057). Black bars represent wild-type cells; open bars represent *cla4-as3 swe1Δ* cells; grey bars represent *cla4-as3 swe1Δ* cells treated with 25 μM 1NM-PP1 for 3 h. **b**, Corresponding F-actin (rhodamine-phalloidin) and DNA (DAPI) staining of 1NM-PP1-treated asynchronous *cla4-as3 swe1Δ* cells. Frame 1, cells 1 h after exposure to inhibitor; frame 2, a cell 3 h after exposure. Scale bar represents 0.75 μm. **c**, Percentage of cells with buds in elutriated *cla4-as3 swe1Δ* cells released into varying concentrations of 1NM-PP1. *n* = 200 cells for all conditions. Circles represent untreated cultures; squares represent cultures treated with 5 μM 1NM-PP1; crosses represent cultures treated with 25 μM 1NM-PP1; triangles represent cultures treated with 50 μM 1NM-PP1. **d**, Percentage of cells with multiple

nuclei (≥3 nuclei per cell) in elutriated *cla4-as3 swe1Δ* cells released into 50 μM 1NM-PP1 (circles) or into medium lacking inhibitor (diamonds). Squares represent multibudded cells in *cla4-as3 swe1Δ* cultures released into medium lacking inhibitor; triangles represent multibudded cells *cla4-as3 swe1Δ* cultures released into 50 μM 1NM-PP1. **e**, Localization of F-actin, Cdc11p (septin) and DNA (DAPI) in unbudded *cla4-as3 swe1Δ* cells released into 50 μM 1NM-PP1 (lower panels) or into medium lacking inhibitor (upper panels) 2.5 h after release from synchrony. Scale bar represents 0.75 μm. **f**, Localization of F-actin, Cdc11p (septin) and DNA (DAPI) in budded *cla4-as3 swe1Δ* cells released into 50 μM 1NM-PP1 (lower panels) or into medium lacking inhibitor (upper panels). Untreated *cla4-as3 swe1Δ* cells were examined 3 h after release from synchrony; treated cells were examined 4 h after release. Scale bars represent 1 μm.

an increase in the fraction of pear-shaped cells in inhibitor-treated cultures that, although not actually budded, appeared to be growing in a polarized fashion (data not shown). The majority of cells ultimately formed buds (Fig. 5c). At later times, we observed a marked increase in the fraction of multinucleated and multiply budded cells in inhibitor-treated cultures, which is consistent with failure of cytokinesis (Fig. 5d).

Addition of 1NM-PP1 to *cla4-as3 swe1Δ* cells did not result in continuous polarization of F-actin or septin to bud tips, as seen in *cla4-as3* cells. Rather, F-actin was polarized to the daughter bud and Cdc11p was localized to bud necks of most cells, forming a complete band around the neck (Fig. 5f). The bud necks of inhibitor-treated *cla4-as3 swe1Δ* cells were frequently abnormal, although defects were heterogeneous (Fig. 5f, asterisk). These results indicate that polarization of both septin and F-actin to bud tips of 1NM-PP1-treated *cla4-as3* cells may require the function of

Swe1p, and that localization of septins to bud necks does not require full Cla4 kinase activity. Nuclear division was evident in inhibitor-treated *cla4-as3 swe1Δ* cells that had small buds or abnormal buds (Fig. 5f), indicating an absence of cell-cycle arrest.

Reversibility of Cla4p inhibition. Arrest caused by chemical inhibition of Cla4p was reversible. We transferred 1NM-PP1-treated *cla4-as3* cells to medium lacking 1NM-PP1 and observed an enlargement of the tips of elongated buds within 20 min. One hour after removal of the drug, most cells had two pronounced, round cell bodies linked by a narrow bridge (Fig. 6a; 67/100 cells). After removal of 1NM-PP1, septin staining appeared to coalesce into a band at bud tips (data not shown). A round bud then grew beyond this septin band; F-actin concentrated within this round bud (Fig. 6b). Nuclear division occurred after this bud reached the approximate size of a normal daughter bud, and we observed long mitotic spindles spanning the length of the unusual cell (Fig. 6b). The *HSL7*-encoded protein,

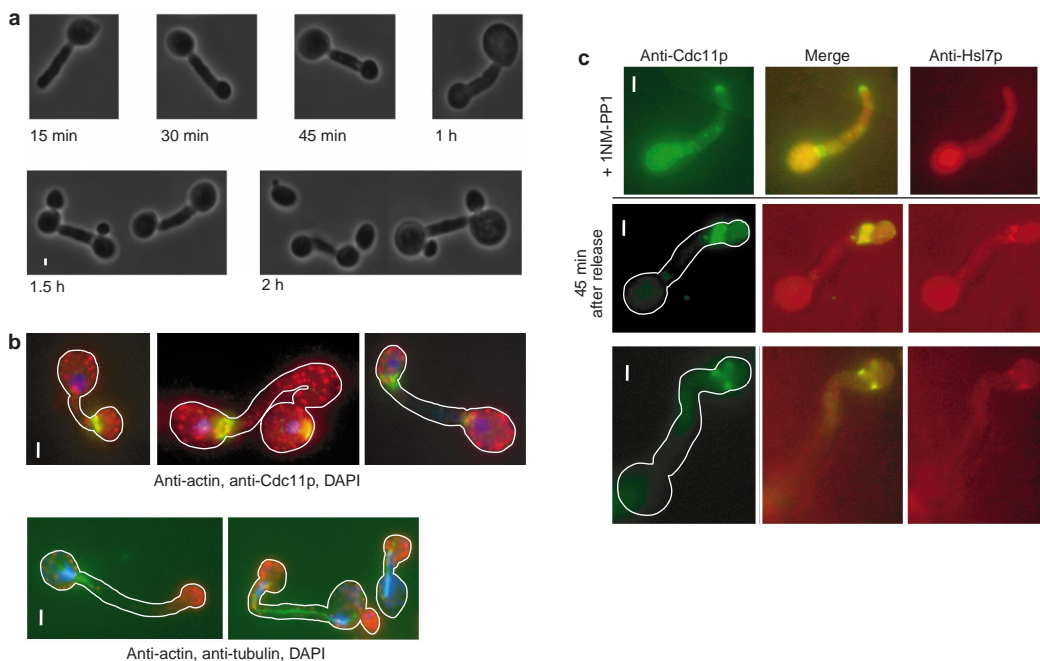


Figure 6 Reversibility of Cla4p inhibition. **a**, Phase-contrast images of 1NM-PP1-treated *cla4-as3* cells at the indicated times after removal of inhibitor. Cells were treated with 1NM-PP1 for 3 h before release and then washed into YPD medium in the absence of inhibitor. Scale bar represents 1 μ m. **b**, Organization of F-actin, septin, and DNA in 1NM-PP1-treated *cla4-as3* cells 1 h after removal of 1NM-PP1. Upper panels, composite of actin (anti-actin), septin (anti-Cdc11p) and DNA (DAPI) staining; lower panels, composite of tubulin (anti-tubulin), actin (anti-actin)

and DNA (DAPI) staining. Leftmost cells have single nuclei; other cells have two. Scale bars represent 1.5 μ m. **c**, Organization of septin and Hsl7p in 1NM-PP1-treated *cla4-as3* cells before and 1 h after removal of 1NM-PP1. Upper panels, septin (anti-Cdc11p) and Hsl7p (anti-Hsl7p) immunofluorescence staining in 1NM-PP1-treated *cla4-as3* cells. Images are composites of two focal planes. Middle and lower panels, localization of septin and Hsl7p 1 h after removal of 1NM-PP1. Scale bars represent 1.5 μ m.

which is part of a protein complex that localizes to bud necks and has been proposed to negatively regulate Swe1p at this site^{29,30}, became co-localized with septin-filament structures only after removal of 1NM-PP1 (Fig. 6c). Recovery from inhibitor treatment was not accompanied by marked changes in levels of Cla4p or by full reversion of the protein to a form with greater electrophoretic mobility (data not shown). Interestingly, cytokinesis and cell separation did not occur at the new bud neck that was formed after removal of 1NM-PP1. Rather, linked cells went on to form daughter buds (Fig. 6a, b). Restoration of Cla4p activity seems to allow formation of a bud neck that cannot serve as a site for cytokinesis but can recruit Hsl7p, perhaps thereby overcoming the checkpoint arrest.

Discussion

We have shown that amino-acid substitutions within the ATP-binding site of the yeast PAK-family kinase Cla4p confer specific sensitivity to the PP1 derivative 1NM-PP1, creating a new type of conditional allele with a relatively well defined biochemical effect. In contrast to techniques that rely on protein depletion, which do not allow discrimination between the functions of different protein domains, allele-specific inhibition of the kinase activity of Cla4p has allowed us to examine the function of a specific protein activity in cell polarization, bud morphogenesis and cytokinesis. Furthermore, this approach avoided the significant complicating factors introduced by temperature shift. Together, our observations indicate that inhibition of Cla4p kinase activity affects bud morphogenesis at or before an early stage of bud emergence, and that this activity may not be required for G1 cell polarization, bud emergence and continuous polarization of F-actin. Furthermore, although it is clear that the full kinase activity of Cla4p is required for formation of a functional cytokinesis site at the mother-daugh-

ter bud neck, these results indicate that Cla4p activity may not be required for cytokinesis once the bud has formed. It has previously been shown that the *in vitro* kinase activity of immunoprecipitated Cla4p is increased as cells proceed into mitosis¹¹; the results presented here indicate that this activity may not reflect the essential *in vivo* function of the kinase. Furthermore, although this PAK activity may recruit important components to the septin ring during its deposition or otherwise affect the organization of this structure, it seems unlikely that Cla4p activity is required for simple localization of septins to the bud neck.

The phenotype caused by Cla4p inhibition in checkpoint-defective *swe1Δ* cells may provide clues to the activities regulated by Swe1p when processes that are important for bud emergence are disrupted. We found that cell-cycle arrest with unusual polarization of both septins and F-actin is *SWE1*-dependent, which is consistent with the proposed function of this gene product as a regulator of a cell-cycle checkpoint that monitors daughter-cell morphogenesis³¹. The unusual organization of both septins and F-actin in inhibitor-treated *cla4-as3* cells indicates that Swe1p may act to prolong processes that are involved in bud emergence in response to the defects caused by reduction of Cla4 kinase activity. Interestingly, we also found that Cla4p inhibition only resulted in a pronounced delay in bud emergence in *swe1Δ* cells. It is therefore possible that Swe1p has a direct function in an adaptive response to defects caused by Cla4p inhibition, activating PAK-independent mechanisms that ensure bud emergence. This would be consistent with the functions of other cell-cycle checkpoints, which both negatively regulate cell-cycle progression and initiate repair responses when critical processes are disrupted³². Although the delay in budding in inhibitor-treated *cla4-as3 swe1Δ* cells was not due to outright failure of cell polarization, Cla4p activity seems to be important for focusing polarization of the actin cytoskeleton to a very small region of the mother-cell cortex.

Septins were present at the bud necks of 1NM-PP1-treated *swe1Δ cla4-as3* cells, indicating that placement of septins at this site may be independent of the kinase activity of Cla4p. This is in contrast to extensive analysis of septin localization in *cla4Δ* cells, which forms the basis of a hypothesis that this PAK regulates the placement of septin filaments at the bud neck. However, the latter analysis is complicated by the necessary presence of the kinase encoded by *STE20*, which normally mediates the very different cortical cytoskeleton organization that underlies the formation of mating projections. There is no direct evidence that Ste20p normally functions in morphogenesis of the emerging bud, and defects in septin organization observed in *cla4Δ* cells may simply stem from the reliance of cells on a PAK that normally carries out a different function. Septin organization at the bud necks of inhibitor-treated *swe1Δ cla4-as3* cells was heterogeneous; this may indicate a function of Cla4p in organizing septin filaments, or it may be a secondary effect arising from defects in an underlying structure or an earlier morphogenetic event. We favour the latter explanation — as cytokinesis occurs in cells that have highly aberrant septin organization^{7,8}, abnormal septin structures seem to be an unlikely explanation for the cytokinetic defect observed in 1NM-PP1-treated *swe1Δ cla4-as3* cells. Identification of the targets of Cla4p should help to resolve the question of whether this kinase has a direct function in septin organization.

Several lines of evidence indicate that PAK kinases have a critical function in cell polarization, which is consistent with their roles as Cdc42p effectors². In the case of Cla4p, this function may include an activating phosphorylation of the type I unconventional myosins Myo3p and Myo5p, although these are almost certainly not the only essential substrates of this kinase^{33,34}. However, we found no evidence that inhibition of the kinase activity of Cla4p blocks actin polarization. In fact, the persistent polarization of F-actin seen in inhibitor-treated *cla4-as3* cells indicates that full activity of the kinase may not be essential for polarization of the actin cytoskeleton. This does not rule out a direct function of this PAK in the formation of cell polarity. If, for example, very little phosphorylation of Myo3/5p by Cla4p is required for actin polarization, 1NM-PP1 may not inhibit the *cla4-as3* protein sufficiently to eliminate this activity. Alternately, type I myosin phosphorylation may not be required for the generation of actin polarization *per se*, but for subsequent processes such as morphogenesis of the bud neck.

Cla4p may have cell-polarization functions that are partially independent of its kinase activity. In accordance with this possibility, overexpression of an N-terminal Cla4p fragment that lacks the kinase domain suppresses a *cdc24* allele that is defective in cell polarization; this suppression is enhanced by concurrent overexpression of Cdc42p¹⁹. It is conceivable that the two domains of the protein normally work in concert upon binding of Cdc42p, with the N-terminal domain recruiting cytoskeleton-organizing factors that are phosphorylated by the C-terminal kinase domain. In accordance with this possibility, the non-kinase N-terminal domain of Cla4p contains at least three motifs that are potentially capable of binding to SH3 domains, which are found in several proteins that are important in cytoskeleton organization, including Abp1p, Bem1p and Myo3/5p^{35,36}. Further genetic analysis of the PAK encoded by *CLA4* may reveal distinct functions of different regions of the protein.

Note added in proof: Alleles with similar effects to *cla4-as1* and *cla4-as2* have been constructed for the well-characterized yeast protein kinases Cdc28p and Fus3p by Bishop *et al.* (A chemical switch for inhibitor-sensitive alleles of any protein kinase. *Nature* 407 395–401; 2000). □

Methods

Plasmid constructions.

YEplac24-*CLA4* and pRS316-*STE20* plasmids were as described^{9,10}. Plasmids carrying inhibitor-sensitive *cla4* alleles and the *cla4^{D693A}* allele were constructed using a Stratagene QuickChange mutagenesis kit according to the manufacturer's instructions. We constructed the *cla4-as1* allele in YEplac24-*CLA4*

using an oligonucleotide of the sequence 5'-GACCTATGGGTTGTGGGGAATTCATGGAAGGAG-GTGGTTC, and its complement, the *cla4-as2* allele in YEplac24-*CLA4* using an oligonucleotide of the sequence 5'-GACCTATGGGTTGTGGCGGAGTTTATGGGAAGG and its complement, and the *cla4-as3* allele in YEplac24-*cla4-as3* using an oligonucleotide of the sequence 5'-CTTGCTGGACACTAGAG-CACGCGTGAATAATGGCGATTTTGGGTTTGGCG and its complement. We sequenced the entire open reading frame *CLA4* of each construct to verify that only the desired substitutions were introduced. We constructed the *cla^{D693A}* allele using an oligonucleotide of the sequence 5'-CAAGCATAT-CATTCATAGCGCTATTAATCAGATAATGTC and its complement. We constructed a ts-degron-tagged *cla4-75* construct essentially as described¹⁵, using the *cla4-75* ORF derived from a plasmid provided by F. Cvrcova¹⁰. This construct was integrated at the *ura3-1* locus as described¹⁵.

Growth conditions, inhibitor treatment and cell-cycle synchronization.

Media and genetic techniques were as previously described⁹⁷. We used nonselective medium (YPD) containing 2% dextrose (Fisher), 1% yeast extract (Difco) and 2% bacto-peptone (Difco) for growth of all *cla4-as* strains after their construction. The inhibitor 1NM-PP1 was prepared as described²⁰ and added to medium to the indicated concentrations from a 25 μM stock in anhydrous dimethylsulphoxide (DMSO, Aldrich) before addition of yeast cells. The final concentration of DMSO in all experimental and control cultures was 0.2%. To generate growth curves for calculation of doubling times, we fixed samples by addition of formaldehyde to 3.7% and determined cell density using a Coulter ZM cell counter. Cells were synchronized in S phase by treatment of exponentially dividing cultures with 0.1 M hydroxyurea in YPD at 25 °C until >90% of cells had large buds (~3 h of treatment). Unbudded cells from stationary-phase cultures were obtained as described²⁶. Centrifugal elutriation was carried out at 4 °C using a Beckman elutriator as recommended by the manufacturer and cultures were grown to an absorbance of $A_{600} = 0.7$ in liquid medium containing 2% raffinose (Difco) as the sole carbon source. Elutriation and fraction collection was carried out at 4 °C. Fractions containing >99% unbudded cells were pooled, collected by filtration and resuspended in YPD + 2% dextrose at 25 °C with the indicated concentrations of 1NM-PP1.

Immunoblotting, immunoprecipitation and protein kinase assays.

Rabbit anti-Cla4p antibodies were provided by H. Tjandra and D. Kellogg. Immunoblotting was carried out as described³⁸ using anti-Cla4p primary antibodies and horseradish-peroxidase (HRP)-conjugated goat anti-rabbit secondary antibodies (Cappel Organon Technika). Immunoblotting against haemagglutinin (HA) was carried out using the HA.11 monoclonal antibody directed against the HA epitope tag (Covance) and horseradish peroxidase conjugated goat anti-mouse secondary antibodies (Cappel Organon Technika). Anti-tubulin immunoblots were performed using YOL134 rat anti-tubulin (Accurate Chemical and Scientific) and HRP-conjugated goat anti-rat secondary antibodies (Cappel Organon Technika). Secondary antibodies were detected using enhanced chemiluminescence (Amersham) and Kodak X-omat AR film pre-flashed twice with a Vivitar flash unit equipped with a number 5 Wratten filter (Eastman Kodak).

Immunoprecipitations of Cla4p were carried out essentially as described²⁴. After washing, 30% of each immunoprecipitation was used for immunoblotting, and each remainder was split into 14 roughly equal fractions to allow duplicate reactions at 7 different concentrations of 1NM-PP1. Before addition of 30 μl reaction buffer (1.5 μg myelin basic protein (Sigma), 5 μM ATP, 20 μCi γ -³²P-ATP (3000 mCi μM⁻¹, New England Nuclear) and the indicated 1NM-PP1 concentrations), immunoprecipitates were washed once in kinase buffer lacking ATP and myelin basic protein but containing the appropriate concentrations of 1NM-PP1. Kinase assays were allowed to proceed for 40 min at 25 °C. Reactions were then stopped with 2 × denaturing sample buffer and run on discontinuous 17.5% SDS-polyacrylamide gels³⁹; bands of myelin basic protein were excised from these gels and incorporation of ³²P was quantified by liquid-scintillation counting of ³²P β-particle emission using a Beckman scintillation counter.

Microscopy, image analysis, F-actin staining and immunofluorescence.

We carried out light microscopy and image capture using a Nikon TE300 inverted microscope equipped with a 100× Plan-Apo/1.4 objective lens and an Orca-100 cooled charge-coupled-device camera (Hamamatsu). Images were acquired as 8-bit grayscale files using Phase 3 image-analysis software; images were subsequently processed using Adobe Photoshop software. Cell outlines were traced using an overlaid phase image as a guide. We stained F-actin with rhodamine-phalloidin (Molecular Probes) using previously described methods⁴⁰. We carried out anti-actin immunofluorescence analysis as described⁴¹, using guinea pig anti-actin primary antibody, anti-tubulin immunofluorescence analysis using YOL134 rat anti-tubulin (Accurate Chemical and Scientific), anti-septin immunofluorescence analysis using rabbit anti-Cdc11p, and anti-Hsl7 immunofluorescence analysis using polyclonal mouse anti Hsl7p. Cy3-conjugated sheep anti-rabbit, Texas-Red-conjugated goat anti-rat, Texas-Red-conjugated donkey anti-mouse (all Sigma), FITC-conjugated donkey anti-rabbit, FITC-conjugated donkey anti-guinea pig (both Cappel/Organon Technika Inc.) were used as secondary antibodies. Single cells were manipulated using a Nikon microscope equipped with a ×20 long working distance objective lens and a Narashige micromanipulator.

RECEIVED 17 APRIL 2000; REVISED 27 JUNE 2000; ACCEPTED 3 JULY 2000;

PUBLISHED 21 SEPTEMBER 2000

- Hall, A. Rho GTPases and the actin cytoskeleton. *Science* 279, 509–514 (1998).
- Bagrodia, S. & Cerione, R. A. Pak to the future. *Trends Cell Biol.* 9, 350–355 (1999).
- Adams, A. E., Johnson, D. I., Longnecker, R. M., Sloat, B. F. & Pringle, J. R. CDC42 and CDC43, two additional genes involved in budding and the establishment of cell polarity in the yeast *Saccharomyces cerevisiae*. *J. Cell Biol.* 111, 131–142 (1990).
- Kozminski, K. G., Chen, A. J., Rodal, A. A. & Drubin, D. G. Functions and functional domains of the GTPase Cdc42p. *Mol. Biol. Cell* 11, 339–354 (2000).
- Field, C. M. & Kellogg, D. Septins: cytoskeletal polymers or signalling GTPases? *Trends Cell Biol.* 9, 387–394 (1999).
- Longtine, M. S. *et al.* The septins: roles in cytokinesis and other processes. *Curr. Opin. Cell Biol.* 8, 106–119 (1996).
- Longtine, M. S., Fares, H. & Pringle, J. R. Role of the yeast Gin4p protein kinase in septin assembly and the relationship between septin assembly and septin function. *J. Cell Biol.* 143, 719–736 (1998).

8. Frazier, J. A. *et al.* Polymerization of purified yeast septins: evidence that organized filament arrays may not be required for septin function. *J. Cell Biol.* **143**, 737–749 (1998).
9. Peter, M., Neiman, A. M., Park, H. O., van Lohuizen, M. & Herskowitz, I. Functional analysis of the interaction between the small GTP binding protein Cdc42 and the Ste20 protein kinase in yeast. *EMBO J.* **15**, 7046–7059 (1996).
10. Cvrckova, F., De Virgilio, C., Manser, E., Pringle, J. R. & Nasmyth, K. Ste20-like protein kinases are required for normal localization of cell growth and for cytokinesis in budding yeast. *Genes Dev.* **9**, 1817–1830 (1995).
11. Benton, B. K., Tinkelenberg, A., Gonzalez, I. & Cross, F. R. Cla4p, a *Saccharomyces cerevisiae* Cdc42p-activated kinase involved in cytokinesis, is activated at mitosis. *Mol. Cell Biol.* **17**, 5067–5076 (1997).
12. Leberer, E., Dignard, D., Harcus, D., Thomas, D. Y. & Whiteway, M. The protein kinase homologue Ste20p is required to link the yeast pheromone response G-protein beta gamma subunits to downstream signalling components. *EMBO J.* **11**, 4815–4824 (1992).
13. Martin, H., Mendoza, A., Rodriguez-Pachon, J. M., Molina, M. & Nombela, C. Characterization of *SKM1*, a *Saccharomyces cerevisiae* gene encoding a novel Ste20/PAK-like protein kinase. *Mol. Microbiol.* **23**, 431–444 (1997).
14. Eby, J. J. *et al.* Actin cytoskeleton organization regulated by the PAK family of protein kinases. *Curr. Biol.* **8**, 967–970 (1998).
15. Holly, S. P. & Blumer, K. J. PAK-family kinases regulate cell and actin polarization throughout the cell cycle of *Saccharomyces cerevisiae*. *J. Cell Biol.* **147**, 845–856 (1999).
16. Delley, P. A. & Hall, M. N. Cell wall stress depolarizes cell growth via hyperactivation of *RHO1*. *J. Cell Biol.* **147**, 163–174 (1999).
17. Brown, J. L., Jaquenoud, M., Gulli, M. P., Chant, J. & Peter, M. Novel Cdc42-binding proteins Gic1 and Gic2 control cell polarity in yeast. *Genes Dev.* **11**, 2972–2982 (1997).
18. Chen, G. C., Kim, Y. J. & Chan, C. S. The Cdc42 GTPase-associated proteins Gic1 and Gic2 are required for polarized cell growth in *Saccharomyces cerevisiae*. *Genes Dev.* **11**, 2958–2971 (1997).
19. Bi, E. *et al.* Identification of novel, evolutionarily conserved Cdc42p-interacting proteins and of redundant pathways linking Cdc24p and Cdc42p to actin polarization in yeast. *Mol. Biol. Cell* **11**, 773–793 (2000).
20. Bishop, A. C. *et al.* Design of allele-specific inhibitors to probe protein kinase signaling. *Curr. Biol.* **8**, 257–266 (1998).
21. Liu, Y., Shah, K., Yang, F., Witucki, L. & Shokat, K. M. Engineering Src family protein kinases with unnatural nucleotide specificity. *Chem. Biol.* **5**, 91–101 (1998).
22. Liu, Y. *et al.* Structural basis for selective inhibition of Src family kinases by PP1. *Chem. Biol.* **6**, 671–678 (1999).
23. Schindler, T. *et al.* Crystal structure of Hck in complex with a Src family-selective tyrosine kinase inhibitor. *Mol. Cell* **3**, 639–648 (1999).
24. Tjandra, H., Compton, J. & Kellogg, D. Control of mitotic events by the Cdc42 GTPase, the Clb2 cyclin and a member of the PAK kinase family. *Curr. Biol.* **8**, 991–1000 (1998).
25. Ayscough, K. R. *et al.* High rates of actin filament turnover in budding yeast and roles for actin in establishment and maintenance of cell polarity revealed using the actin inhibitor latrunculin-A. *J. Cell Biol.* **137**, 399–416 (1997).
26. Johnston, L. H. & Johnson, A. L. Elutriation of budding yeast. *Methods Enzymol.* **283**, 342–350 (1997).
27. Dohmen, R. J., Wu, P. & Varshavsky, A. Heat-inducible degron: a method for constructing temperature-sensitive mutants. *Science* **263**, 1273–1276 (1994).
28. Lew, D. J. & Reed, S. I. A cell cycle checkpoint monitors cell morphogenesis in budding yeast. *J. Cell Biol.* **129**, 739–749 (1995).
29. McMillan, J. N. *et al.* The morphogenesis checkpoint in *Saccharomyces cerevisiae*: cell cycle control of Swe1p degradation by Hsl1p and Hsl7p. *Mol. Cell Biol.* **19**, 6929–6939 (1999).
30. Shulewitz, M. J., Inouye, C. J. & Thorner, J. Hsl7 localizes to a septin ring and serves as an adapter in a regulatory pathway that relieves tyrosine phosphorylation of Cdc28 protein kinase in *Saccharomyces cerevisiae*. *Mol. Cell Biol.* **19**, 7123–7137 (1999).
31. Lew, D. J. Cell-cycle checkpoints that ensure coordination between nuclear and cytoplasmic events in *Saccharomyces cerevisiae*. *Curr. Opin. Genet. Dev.* **10**, 47–53 (2000).
32. Elledge, S. J. Cell cycle checkpoints: preventing an identity crisis. *Science* **274**, 1664–1672 (1996).
33. Wu, C., Lytvyn, V., Thomas, D. Y. & Leberer, E. The phosphorylation site for Ste20p-like protein kinases is essential for the function of myosin-I in yeast. *J. Biol. Chem.* **272**, 30623–30626 (1997).
34. Lechler, T., Shevchenko, A. & Li, R. Direct involvement of yeast type I myosins in Cdc42-dependent actin polymerization. *J. Cell Biol.* **148**, 363–373 (2000).
35. Chenvert, J., Corrado, K., Bender, A., Pringle, J. & Herskowitz, I. A yeast gene (*BEM1*) necessary for cell polarization whose product contains two SH3 domains. *Nature* **356**, 77–79 (1992).
36. Drubin, D. G., Mulholland, J., Zhu, Z. M. & Botstein, D. Homology of a yeast actin-binding protein to signal transduction proteins and myosin-I. *Nature* **343**, 288–290 (1990).
37. Guthrie, C. & Fink, G. R. (eds) *Guide to Yeast Genetics and Molecular Biology* (Academic, San Diego, 1991).
38. Towbin, H., Staehelin, T. & Gordon, J. Electrophoretic transfer of proteins from polyacrylamide gels to nitrocellulose sheets: procedure and some applications. *Proc. Natl Acad. Sci. USA* **76**, 4350–4354 (1979).
39. Anderson, C. W., Baum, P. R. & Gesteland, R. F. Processing of adenovirus 2-induced proteins. *J. Virol.* **12**, 241–252 (1973).
40. Cope, M. J., Yang, S., Shang, C. & Drubin, D. G. Novel protein kinases Ark1p and Prk1p associate with and regulate the cortical actin cytoskeleton in budding yeast. *J. Cell Biol.* **144**, 1203–1218 (1999).
41. Mulholland, J. *et al.* Ultrastructure of the yeast actin cytoskeleton and its association with the plasma membrane. *J. Cell Biol.* **125**, 381–391 (1994).

ACKNOWLEDGMENTS

We thank H. Tjandra, D. Kellogg, M. Longtine, M. Shulewitz, J. Thorner, F. Cvrckova, S. Holly and K. Blumer for providing essential strains, plasmids, and antibodies, and S. Biggins and J. Li for assistance with elutriation. We also thank J. Ubersax and members of the Drubin and Barnes laboratories, particularly M. J. T. V. Cope, M. Duncan, K. Kozminski and D. Seikhaus, for helpful discussions. E.L.W. is supported by an American Cancer Society postdoctoral fellowship; support for this work was also provided by a grant from the National Institutes of Health (to D.G.D.). Correspondence and requests for materials should be addressed to D.G.D.